JOURNAL OF GEOPHYSICAL RESEARCH, VOL. 102, NO. A11, PAGES 24,037–24,046, NOVEMBER 1, 1997

Storm time dependence of equatorial disturbance dynamo zonal electric fields

Ludger Scherliess and Bela G. Fejer

Center for Atmospheric and Space Sciences, Utah State University, Logan

Abstract. We use Jicamarca radar observations of *F* region vertical plasma drifts and auroral electrojet indices during 1968-1988 to study the characteristics and temporal evolution of equatorial disturbance dynamo zonal electric fields. These electric fields result from the dynamo action of storm time winds and/or thermospheric composition changes driven by enhanced energy deposition into the high-latitude ionosphere during geomagnetically active conditions. The equatorial vertical drift perturbations last for periods of up to 30 hours after large increases in the high-latitude currents. On the average, this process can be described by two basic components with time delays of about 1-12 hours and 22-28 hours between the high-latitude current enhancements and the equatorial velocity perturbations. Our data indicate strong coupling between dynamo processes with different timescales. The short-term disturbance dynamo drives upward equatorial drifts (eastward electric fields) at night with largest amplitudes near sunrise and small downward drifts during the day. These perturbation drifts are in good agreement with results from the Blanc-Richmond disturbance dynamo theory. The dynamo process with time delays of about a day drives upward drift velocities at night with largest values near midnight and downward drifts in the sunrise-noon sector. In this case, the amplitudes of the disturbance drifts maximize during geomagnetically quiet times preceded by strongly disturbed conditions. We also present results of a new equatorial storm time dependent empirical model which illustrate the characteristics of the vertical disturbance dynamo drifts.

I. Introduction

The transport of energy and momentum from the high-latitude ionosphere to lower latitudes has long been known to strongly affect the middle- and low-latitude thermosphere. Solar wind-magnetospheric disturbances give rise to equatorward propagating neutral wind surges and gravity waves and to global ionospheric electric field and current perturbations. These processes can alter significantly the global thermospheric circulation and the ionization density and composition, particularly at *F* region altitudes, over periods of days [e.g., *Fuller-Rowell et al.*, 1994, 1996; *Prölss*, 1995]. The understanding of these transport processes during geomagnetically active conditions is of fundamental importance for the development of realistic global thermospheric, ionospheric and protonospheric models.

Studies of storm time ionospheric electrodynamics have shown the occurrence of large electric field and current disturbances during and after geomagnetically disturbed periods. Electric field perturbations with timescales of about an hour, occurring nearly simultaneously at all latitudes, have been attributed to the prompt penetration of high-latitude electric fields to lower latitudes. In addition to these sudden perturbations, longer lasting (timescales of a few hours) middle- and low-latitude electrodynamic disturbances often occur from a few to several hours after large enhancements in the high-latitude currents [e.g., *Fejer et al.*, 1983; *Fejer*, 1986]. These electric field perturbations are most probably associated with ionospheric disturbance dynamo effects produced by enhanced energy deposition into the auroral ionosphere during geomagnetically active periods [*Blanc and Richmond*, 1980]. Figure 1 illustrates the effects of short- and long-lived electric field disturbances on the equatorial *F* region vertical plasma drifts measured with the Jicamarca incoherent scatter radar during and after a period of large high-latitude current enhancements. It is of interest to note the occurrence of large drift perturbations between about 0500 and 1000 UT on August 10 when the auroral electrojet indices were relatively small. *Fejer et al.* [1983] interpreted these delayed perturbations as due to ionospheric disturbance dynamo electric fields. During strongly disturbed conditions, prompt penetration and disturbance dynamo effects often occur simultaneously, as illustrated between about 0700 and 1000 UT on August 9. This has been a major obstacle for the full validation of the electrodynamic results from global convection and disturbance dynamo models.

Recently, *Fejer and Scherliess* [1995] have presented a new methodology which can separate the effects of the magnetospheric and ionospheric disturbance dynamos and provides considerably more information on the morphology and efficiency of these processes. They showed that the general characteristics of prompt penetration and time-delayed equatorial zonal electric field perturbations are in good agreement with results from global convection [e.g., *Senior and Blanc*, 1984; *Spiro et al.*, 1988; *Denisenko and Zamay*, 1992], and ionospheric disturbance dynamo [*Blanc and Richmond*, 1980] models, respectively. However, the relatively simple empirical model developed by *Fejer and Scherliess* [1995] did not provide detailed information on the storm time dependence of the ionospheric disturbance dynamo electric fields. Here we use extensive *F* region vertical plasma

Paper number 97JA02165.
0148-0227/97/97JA-02165$09.00

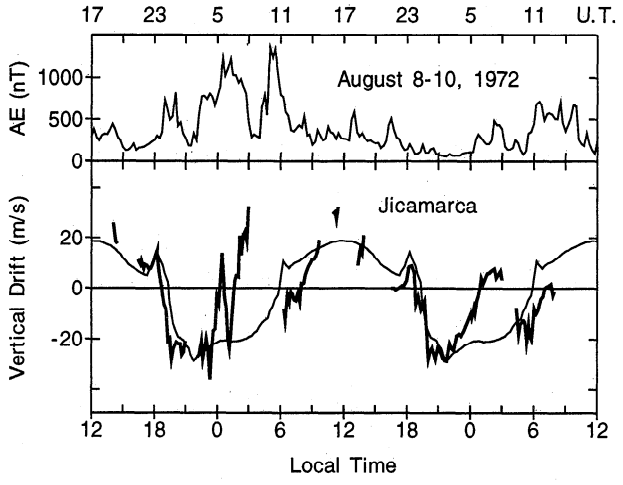

Figure 1. An example of a 48-hour period of large perturbations in the equatorial vertical (positive upward) plasma drifts over Jicamarca, Peru, during a magnetically disturbed period. The thin solid curve corresponds to the average quiet time pattern. The auroral electrojet indices are shown in the top.

drift measurements from the Jicamarca Observatory to determine the basic components of the equatorial disturbance dynamo zonal electric fields. These perturbation electric fields (vertical drifts) are driven by enhanced energy deposition into the high-latitude ionosphere, which can be modeled by using auroral electrojet indices. We also present an analytical empirical model for the disturbance dynamo drifts and compare model results with observations. In a companion paper, *Fejer and Scherliess* [this issue] study prompt penetration electric fields driven by sudden changes in the high-latitude convection, and the response of equatorial vertical drifts to both direct penetration and disturbance dynamo effects.

2. Data Analysis

We study equatorial zonal disturbance electric fields obtained from *F* region vertical plasma drift measurements from the Jicamarca incoherent scatter radar (12.0° S, 76.9° W; magnetic dip 2°N), near Lima, Peru. The radar data used here correspond to average values over an altitude range of about 250-600 km where these drifts are largely height independent. The time resolution is about 5 min, and the accuracy is of the order of 1-2 m/s. The experimental procedure used at Jicamarca for vertical drift measurements was described by *Woodman* [1970]. In the Peruvian equatorial region, an upward *F* region plasma drift of 40 m/s corresponds to an eastward electric field of about 1 mV/m. Our drift database consists of 4926 hours of measurements from 1968 through June 1988. We use the auroral electrojet (*AE*) index to characterize the level of high-latitude geomagnetic activity. This parameter is available with time resolution of minutes and has been empirically related to both the polar cap potential drop and to the hemispheric high-latitude energy input [e.g., *Ahn et al.*, 1983, 1992].

The general procedure we have used for the study of the disturbance electric fields (plasma drifts) was described briefly by *Fejer and Scherliess* [1995] and in more detail by *Fejer and Scherliess* [this issue]. Basically, we first determine the plasma drift perturbations by subtracting the season and solar cycle dependent average quiet time values from the quarter-hourly or, in the present case, from hourly averaged drifts. The resulting perturbations are due to prompt penetration and disturbance dynamo electric fields and to the day-to-day variability of the ionospheric dynamo electric fields. Since our average quiet time drifts correspond to an *AE* index of about 130 nT, we study the disturbance drifts (relative to the corresponding average quiet time values) as a function of AE_d=*AE*−130 nT for positive values of this parameter. These perturbations are then related to corresponding changes in the auroral indices (to account for prompt penetration electric field effects) and also to a time series of auroral indices which define the level of geomagnetic activity for a period of several hours prior to the time of the drift measurements. Since the ionospheric disturbance dynamo electric fields have time constants of a few hours, we have used hourly averaged drifts and *AE* indices. This allows for a fairly simple removal of shorter timescale prompt penetration effects from the perturbation drifts and also reduces the noise in the database.

Following *Fejer and Scherliess* [1995], we studied storm time dependent electric fields using linear regression analysis, simultaneous multiple parameter fitting, and storm time dependent binning. These methods have different strengths and weaknesses, but collectively they provide considerable new insight into the underlying physics and morphology of storm time dynamo processes. Linear regression analysis was used to obtain approximate relationships between equatorial drift perturbations and auroral current enhancements separated by different time delays. *Fejer and Scherliess* [1995] used this method to show that the largest equatorial disturbance dynamo zonal electric fields have time delays of about a few hours. The simple linear regression analysis used here does not provide accurate time dependent relationships between equatorial and auroral disturbances since usually it is unable to completely separate perturbations due to competing processes with different time constants. Simultaneous multiple parameter fitting of the entire perturbation drift database provides the best possible estimate of efficiencies of different storm time processes, but this method requires a priori knowledge of the appropriate fitting parameters and therefore of their approximate time constants. We used linear regression analysis to obtain the most suitable parameters for our simultaneous multiple parameter fitting scheme. Storm time dependent binning, which requires very large databases, was used to determine the basic signatures of the disturbance dynamo mechanism, as well as to examine the agreement of these results and those from our multiparameter empirical model. In the following sections, we show the use of these three methods, determine the basic signatures and time constants of the different components of the disturbance dynamo zonal electric fields, present an empirical model for these perturbation electric fields, and finally, illustrate the use of this model for case studies.

3. Results

We studied the time dependent efficiency of the disturbance dynamo by binning initially the perturbation vertical drifts, $v(t)$, as a function of $AE_d(t-\tau) > 0$, where t is local time and τ = 1 - 72 hours is the time delay between the auroral and equatorial perturbations. Since the disturbance dynamo processes have time constants of a few hours and longer, we combined these data in 3-hour sliding local time and time delay

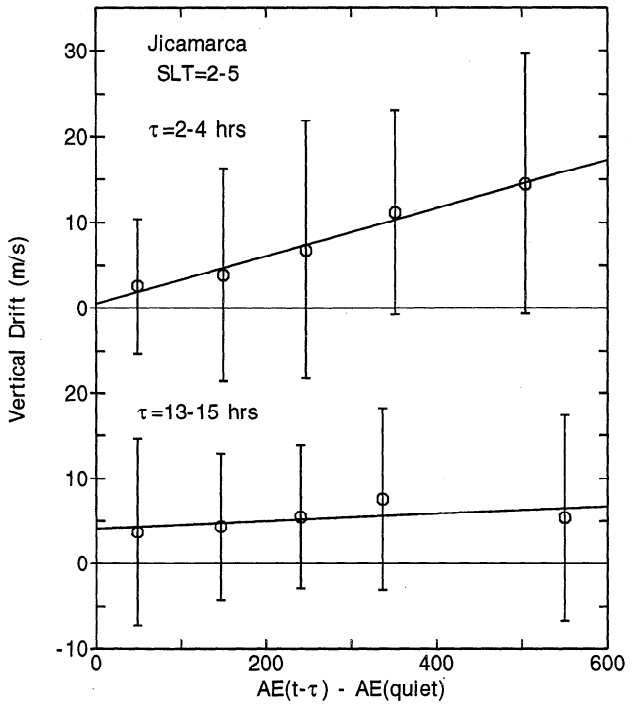

Figure 2. Examples of the relationship between nighttime equatorial vertical plasma drifts and time delayed auroral electrojet indices. Here τ denotes the time delay between the auroral and equatorial disturbances.

intervals centered on the half hour. The drifts were binned in 100 nT windows of $AE_d(t-\tau)$ up to 400 nT, and into a single bin for larger values. Then, for each time delay, a linear regression analysis was performed using the average drifts and AE_d indices computed in each bin. We used average values instead of individual data points for the linear regression analysis since there is a significantly larger number of drift measurements during periods when the AE_d indices are small. Figure 2 shows results from this linear regression analysis for two periods of time delays between high-latitude and equatorial disturbances.

The regression analysis gives a straight line, $v(t,AE) = v_0+S\cdot AE_d(t-\tau)$, where v_0 is the offset value and S is the slope and also the sample correlation coefficient R. The offset value can be interpreted as due to the cumulative effect of perturbations with time delays different from the one under consideration, whereas the slope relates the amplitudes of the velocity perturbations to the corresponding AE_d values. The linear correlation coefficient R is a measure of the total variation of the perturbation drifts which is accounted for by the derived relationship between $v(t,AE)$ and $AE_d(t-\tau)$ [*Freund and Walpole*, 1987; *Reiff*, 1990] . More rigorously, it is defined as the square root of the fraction of the variance that is explainable by the linear fit. Since $(1-R^2)$ is the fraction of the variance that remains after the linear correlation, we will use below R^2S as a measure of the relative dependence of the perturbation drifts on the auroral current enhancements, as measured by $AE_d(t-\tau)$. The values of the correlation coefficients obtained in our analysis depend strongly on the AE binning. For our bin size of 100 nT, we have absolute values of the correlation coefficient of up to 0.9 indicating that on the average, the day-to-day variability (unrelated to high-latitude current conditions) is basically canceled out. The use of smaller bin sizes reduces the number of points per bin and decreases the sample correlation coefficients, which reflects increased effects from day-to-day variability.

The regression analysis described above cannot effectively separate disturbance dynamo effects with significantly different time delays. Therefore we have applied this method using a two-step process. In the first, we have determined that AE_d enhancements affect the equatorial vertical drifts only for time delays shorter than about 35 hours. In the second, we have minimized the contamination between short- (less than 12 hours) and long-term (longer than 20 hours) dynamo effects by deleting from the regression analysis (but not from the multiparameter fitting analysis to be described later) drifts associated with both short- and long-term disturbed conditions (average AE_d > 170 nT, and hourly values > 370 nT). For example, to determine the efficiency of the disturbance dynamo for an average time delay $\tau = 5$ hours, we deleted from the analysis drift data associated with significantly enhanced auroral activity between about 15-20 and 35 hours earlier. For time delays longer than about 20 hours, we used only drifts measured following about 12 hours of relatively quiet magnetic conditions, as specified above. For intermediate time delays, the analysis was carried out using drifts associated only with our relatively quiet conditions outside a sliding "time window" centered on the time delay under consideration. Several window sizes were used without significant changes in the regression analysis, and we finally decided on a half width of 15 hours. This window size does not exclude long lasting storms and still allows the separation of short- and long-term effects. The results shown in Figure 2 were obtained using this procedure.

Plate 1 shows the temporal dependence of the relative efficiency (slope·R^2 normalized to a maximum value of 1) of the disturbance dynamo equatorial vertical plasma drifts obtained from our regression analysis. Time delays longer than 35 hours are not shown since the corresponding efficiencies are at the noise level (relative efficiencies < 0.15) for all local time sectors. Efficiencies smaller than this value were also set to zero in Plate 1. Our results indicate that the largest values occur in the postmidnight sector where this mechanism generates upward velocity (eastward electric field) perturbations. Figure 3 shows these results in more detail in three local time sectors. The results shown in Plate 1 and Figure 3 are less reliable for time delays smaller than 2 hours since, in this case, it is essentially impossible to completely remove prompt penetration effects. In addition, small fluctuations shown in Figure 3, particularly for time delays between 12 and 20 hours during the day, depend somewhat on the choice of the time window used in the regression analysis. *Fejer* [1997] presented a slightly different version of Figure 3 obtained without the use of a time window. It is also important to notice that the frequent correlation of consecutive AE indices and our use of 3-hour sliding averages cause a temporal broadening of the efficiency patterns.

Plate 1 and Figure 3 show that the largest disturbance dynamo upward drifts (eastward electric fields), which correspond to large positive efficiencies, occur for time delays of a few hours in the postmidnight sector. This is consistent with the conclusions of *Fejer and Scherliess* [1995]. In the postmidnight sector, the disturbance dynamo efficiency varies only slightly for the first ten hours after auroral disturbances, it goes to zero for time delays between about 15 and 19 hours, and has again large positive values for time delays between

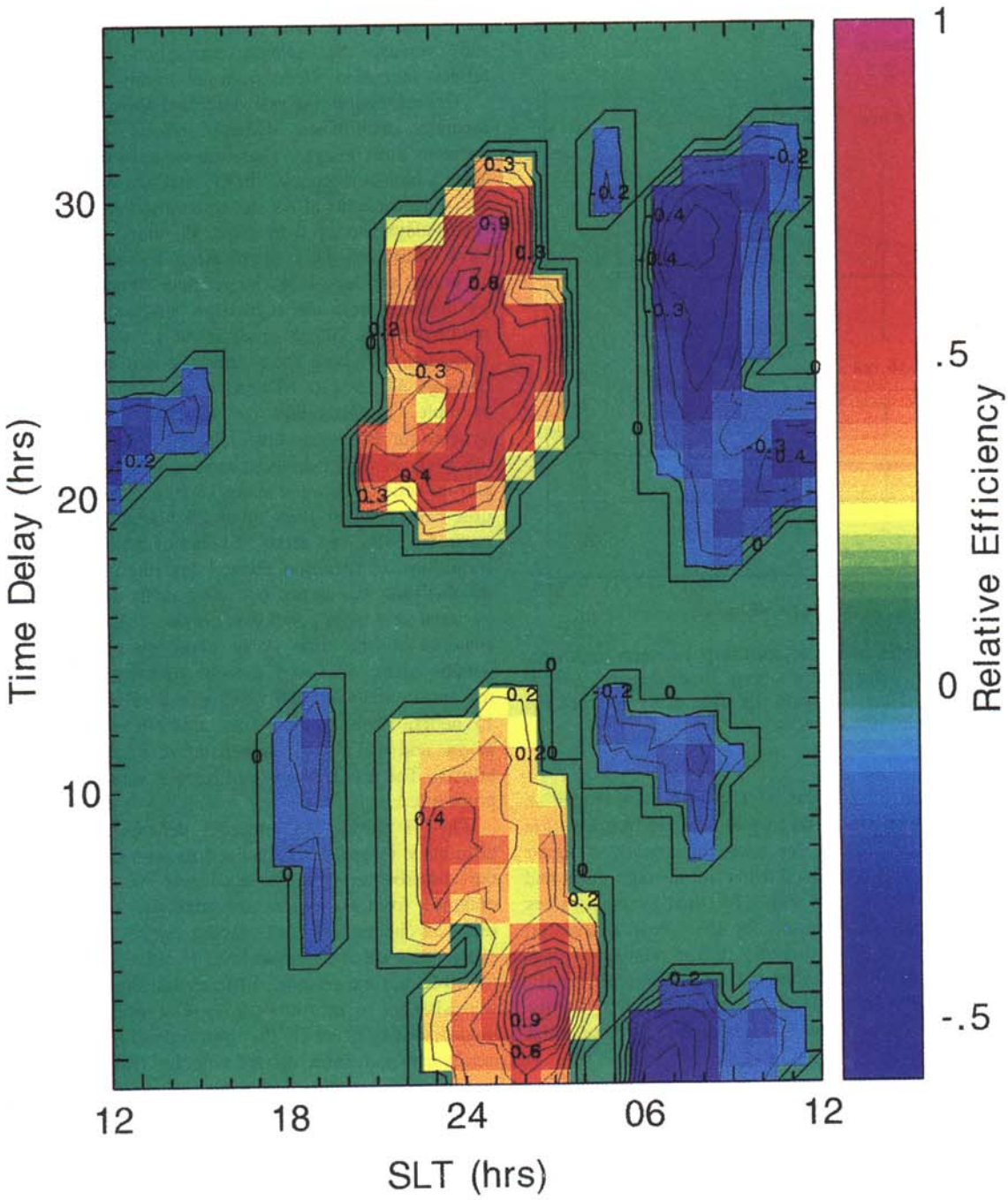

Plate 1. Plot of the efficiency of the disturbance dynamo process for the generation of vertical plasma drifts as a function of local time and time delay between the high-latitude and equatorial disturbances. Positive efficiency corresponds to the generation of upward perturbation drifts (eastward electric fields).

about 20 and 30 hours. In the morning sector, the disturbance drifts are downward (corresponding to negative efficiencies), have smaller amplitudes, and are associated with time delays longer than about a few hours. Figure 3 also shows that ionospheric disturbance dynamo drifts are not seen in the afternoon sector. As mentioned above, our analysis, using *AE* indices and 3-hour sliding averages, does not determine the exact temporal dependence of the equatorial plasma drifts on the high-latitude current perturbations.

We have seen that on the average, the response of the equatorial zonal electric field to high-latitude current enhancements can be roughly separated into short-, intermediate-, and long-term effects with time delays $\tau \approx$ 1-12, 12-20, and 20-30 hours, respectively. Additional information can be obtained by binning the data according to their storm time history. In this way, we are able to distinguish drift responses associated with the growth and recovery phases of the high-latitude current enhancements, as well as to examine possible relationships between ionospheric dynamo effects with different time delays. In the following sections, we examine in more detail the short- and long-term disturbance drifts using storm time binning, linear regression analysis,

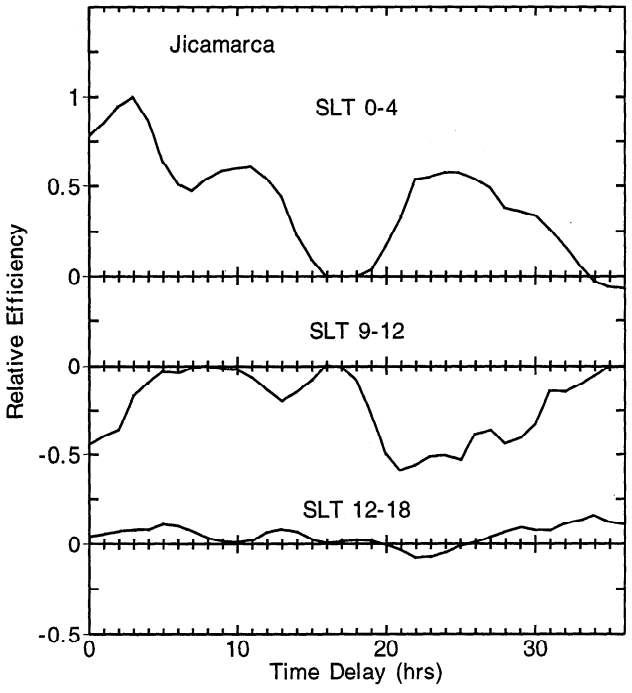

Figure 3. Relative efficiency of the disturbance dynamo process in three local time sectors as a function of the time delay between the auroral and equatorial disturbances.

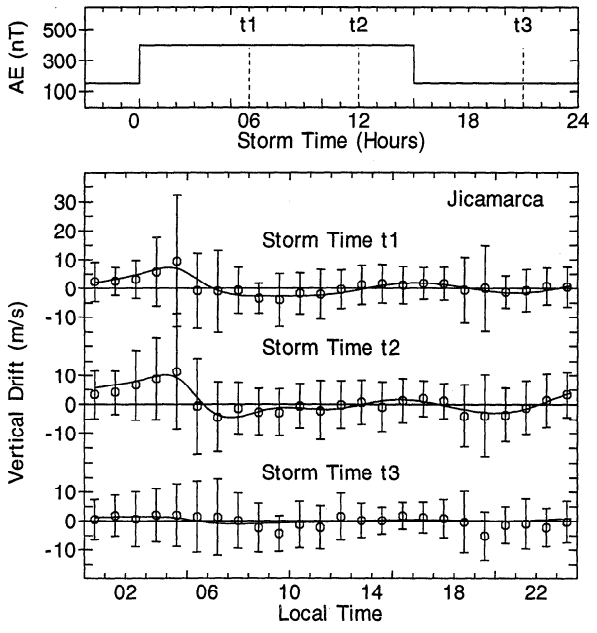

Figure 4. Local time variation of equatorial disturbance dynamo vertical drifts at the storm times shown in the top. The points with the scatter (not error) bars were obtained by binning the data for the conditions in the top, whereas the solid curve is the result from an empirical model for the same conditions.

and a spline-fitted multiparameter model. The use of these analysis techniques will allow us to determine that in general, the amplitudes of the short- and long-term perturbation drifts depend not only on the values of the corresponding auroral indices but also on the storm history.

3.1. Short-Term (τ = 1-12 Hours) Effects

The results above indicate that the response of equatorial vertical drifts to magnetic activity is strongly storm time dependent. This is illustrated further in Figure 4 where the top panel shows an idealized variation of the auroral index and the bottom panel indicates the local time dependent average perturbation drifts at the three storm times. The data points with the scatter bars were obtained by binning the perturbation drifts for the conditions illustrated in the top panel. The binning criteria and the average *AE* indices are given in Table 1. The solid curves show the results obtained from an analytical cubic-B spline model to be described later. The scatter on the data is partly due to our binning criteria, as well as to the remaining day-to-day variability superposed on the disturbance drifts. In addition, although prompt penetration electric field effects do not change the average perturbation drifts shown in Figure 4, since the average ΔAE values are approximately zero, they increase the scatter in the data.

Figure 4 shows upward drift perturbations throughout the night with largest amplitudes in the 2-5 local time sector and smaller downward perturbations during the day, which is in good agreement with the results of *Fejer and Scherliess* [1995]. For the condition shown in the top panel in Figure 4, the nighttime perturbation drifts increase with storm time, and roughly double their amplitudes from t1 to t2. For longer time delays, however, these amplitudes remain essentially constant as suggested by Figure 3. This is an indication that after about 12 hours of constant high-latitude energy input, the nighttime equatorial vertical plasma drifts reach a new equilibrium. The bottom panel in Figure 4 shows that about 6 hours after the end of the period of enhanced *AE* indices the average perturbations are essentially zero at almost all local times, i.e., the vertical drifts have returned to their quiet time values. This time constant for recovery to quiet time values is consistent with that of thermospheric winds following magnetic storms [*Fuller-Rowell et al.*, 1994].

It is interesting to note that the local time average of the disturbance dynamo electric fields is not zero. This is also the case for the quiet time average vertical plasma drifts, as shown by *Fejer et al.* [1979]. They interpreted the latter results as indicative that this atmospheric dynamo process is longitude dependent. On the other hand, the vertical plasma drift perturbations resulting from prompt penetration electric fields average out to zero [*Fejer and Scherliess*, this issue], as suggested by global convection models.

The short-term (τ=1–12 hours) disturbance dynamo process is more complex than suggested above. This mechanism has

Table 1. Binning Criteria and Average Indices

Storm Time	t1	t2	t3	t4
$\overline{AE(01-06 \text{ hours})}$ (nT)	≥ 250(373)	≥ 200(419)	≤ 250(162)	≤ 300(159)
$\overline{AE(07-12 \text{ hours})}$ (nT)	≤ 250(156)	≥ 200(423)	≥ 250(358)	≤ 300(178)
$\overline{AE(22-28 \text{ hours})}$ (nT)	-----	-----	-----	≥ 400(572)

basically two coupled components with τ =1–6 hours and τ = 7–12 hours, although the choice of these periods is somewhat arbitrary. For example, a split into τ = 1–5 hours and τ = 6–12 hours or τ = 1–7 hours and τ = 8–13 hours would have given very similar linear regression results although with smaller correlation coefficients. These two components will allow us to model realistically the recovery to quiet time values as well as the effects of short lasting (few hours) and extended high-latitude disturbances and also to directly compare the corresponding disturbance dynamo efficiencies. The regression analysis indicates that the efficiency of the dynamo process with τ =7-12 hours increases significantly with the average level of magnetic activity in the previous 6 hours, i.e., with *AE*(1-6 hours). This can be seen by noticing that in Figure 4 the incremental effect of *AE*(7-12 hours) essentially doubled the amplitude of the nighttime perturbation drifts at storm time t2 relative to t1, but did not produce any perturbation drifts at storm time t3 when *AE*(1-6 hours) had a much smaller value above our quiet time average.

Blanc and Richmond [1980] studied the characteristics of the ionospheric disturbance electric fields driven by Joule heating in the auroral zone using numerical simulations. *Mazaudier and Venkateswaran* [1990] have used mid-latitude plasma drift and neutral wind measurements and equatorial magnetic field data to examine ionospheric disturbance dynamo effects following a large magnetic storm. In this process, the dissipation of enhanced energy deposition into the high-latitude ionosphere generates a meridional circulation with equatorward winds above about 120 km which, through the action of the Coriolis force, leads to westward winds and plasma drifts. The equatorward Pedersen current generated by the westward ion drifts at altitudes where the cross-field conductivity is high (about 150 km) builds up polarization charges at the equator and a poleward electric field which eventually cancels the equatorward Pedersen current. The resulting eastward Hall current, which maximizes at mid-latitudes, sets up polarization charges at the terminators and a dusk-to-dawn electric field. The equatorial vortex associated with this disturbance current system has the opposite polarity to the quiet time ionospheric dynamo current. It is important to notice that the storm time winds in the Blanc-Richmond model build up steadily at upper mid-latitudes and do not have significant amplitudes near the equator. Therefore, in this model, the time delay between the auroral current enhancements and the equatorial electric field disturbances correspond to the growth time of the mid-latitude storm time wind system.

We can compare the equatorial zonal electric fields predicted by the Blanc-Richmond model with our empirical disturbance patterns by using derived relationships between the hemispheric power input and the *AE* index. Empirical studies [e.g., *Ahn et al.*, 1983; *Mazaudier et al.*, 1987] indicate that the hemispheric Joule heating can be expressed as U_J (MW) = (230 - 400) *AE* (nT). The variability in the proportionality factor is largely due to the different conductivity models used in these studies. Here we use U_J (MW) = 300 *AE* (nT). In this case, an increase in the *AE* index by 400 nT corresponds to an enhanced hemispheric Joule heating which is about a factor of 7 smaller than that used in the case I simulation of *Blanc and Richmond* [1980]. We have scaled down the results from the theoretical model by this factor (even though this model is nonlinear), to allow a direct comparison with our empirical results. Figure 5 illustrates the excellent agreement between the results from the empirical model, the Blanc-Richmond model, and the binned data, for an increased hemispheric Joule heating input corresponding to 400 nT over a period of 9 hours.

In addition to the Blanc-Richmond mechanism, there are also other potentially important storm time ionospheric dynamo processes. This includes the dynamo effects of fast traveling atmospheric disturbances (TADs) which reach equatorial latitudes a few hours after the onset of high-latitude current enhancements [e.g., *Prölss*, 1995; *Fuller-Rowell et al.*, 1994, 1996], of fossil winds equatorward of the shielding layer following rapid poleward motions of the equatorward edge of the diffuse aurora after sudden geomagnetic quieting [*Fejer et al.*, 1990], and of magnetic storm induced conductivity/composition changes. However, the efficiency of these processes in generating ionospheric electric fields still remains to be determined. *Fejer et al.* [1990] suggested that fossil winds could explain the larger and longer lasting equatorial zonal electric field perturbations following large and sudden decreases in high-latitude convection compared to the perturbations associated with convection enhancements of the same magnitude. Although, as discussed in the companion paper by *Fejer and Scherliess* [this issue], it is possible that this mechanism could contribute to the generation of relatively short-term disturbance electric fields following sudden quieting, this asymmetry seems to be largely due to disturbance dynamo effects. In the following section, we describe the characteristics of longer-term disturbance drifts probably generated by a different dynamo mechanism.

3.2. Long-Term (τ = 20-30 Hours) Effects

We have seen that the equatorial plasma drifts are essentially independent of enhancements in the auroral current systems, as measured by the *AE* index, for time delays of about 13-20 hours, but can strongly respond to high-latitude current disturbances occurring about 20-30 hours earlier. We studied the long-term disturbance drifts using a linear regression analysis combined with restrictions on the short-term geomagnetic conditions in order to minimize the mixing of short- and long-term dynamo effects. Our analysis indicates that the highest correlation coefficient between the *AE* indices and the long-term equatorial vertical drifts occurs for time delays of 22 to 28 hours, although slightly different ranges of time delays do not affect the results significantly. These

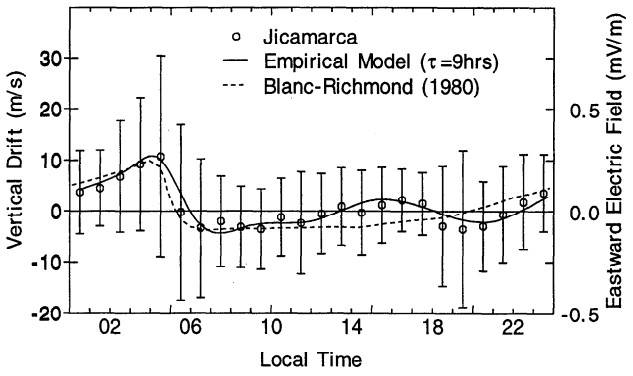

Figure 5. Comparison of the empirical disturbance dynamo drift pattern with the result from the Blanc-Richmond model both for an increase in the hemispheric power input corresponding to about 400 nT over our quiet time level.

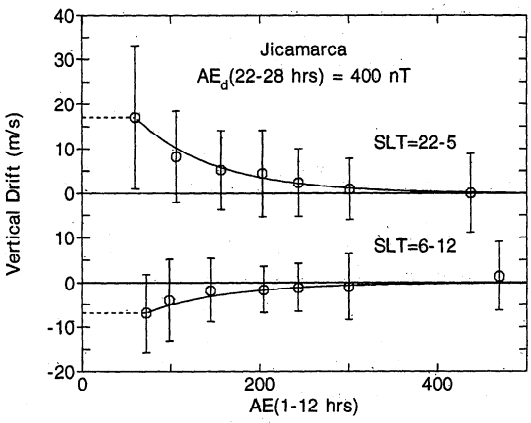

Figure 6. Long-term dynamo perturbation drifts for AE_d = 400 nT as a function of the average short-term auroral electrojet indices. The solid curve indicates the analytical representation used in our model to denote this empirical relationship.

effects are largely restricted to the nighttime and morning sectors and to periods when geomagnetically quiet conditions over several hours are preceded by large or moderate storms (i.e., when the average *AE*(22-28 hours) > 350 nT). Figure 6 shows the local time variation of the long-term disturbance drifts in the nighttime and morning sectors for AE_d(22-28 hours) = 400 nT, as a function of the short-term average *AE*(1-12 hours) value. The solid curve, $\beta \sim \exp[-AE(1-12 \text{ hours})/90$ nT], was obtained by a least squares fit to the data. Figure 6 indicates that the long-term disturbance dynamo drifts are largest under short-term geomagnetically quiet conditions. In this case, our linear correlation analysis indicates that the long-term dynamo drifts are proportional to [AE_d(22-28 hours) - 200 nT] for positive values of this parameter. On the other hand, for *AE*(1-12 hours) > 250 nT, the long-term dynamo drifts are very small although the short-term ones, described earlier, are not. In our empirical model we will use $\beta(AE)$ to account for the effect of the short-term magnetic activity on the efficiency of the long-term dynamo mechanism. Figure 6 shows large variability in the perturbation drifts for geomagnetically quiet short-term conditions. This is due in part to the relatively smaller number of data points which simultaneously satisfy the conditions of large long-term and small short-term average *AE* values. However, it is likely that other effects, such as energy deposition in different local time sectors, which are not accounted for by our use of the *AE* index, also strongly affect the efficiency and the time delay of the long-term disturbance dynamo process.

Figure 7 shows a comparison of the long-term disturbance drift pattern obtained from our empirical model with binned data for long-term disturbed and short-term quiet magnetic conditions. The binning criteria and the average values of these indices are given in Table 1 under storm time t4. In this case, large upward drift perturbations occur during the entire nighttime period with largest amplitudes around 0100 LT. The daytime downward drifts have smaller amplitudes which maximize between about 0700 and 1100 LT. As mentioned above, the long-term disturbance drifts exhibit large variability; the results presented here correspond to an average *AL*/*AU* ≈ 2. Preliminary results suggest that time delays somewhat shorter (longer) than 22-28 hours are associated with *AL*/*AU* ratios larger (smaller) than about 2. Clearly, a more extensive data set is needed to fully characterize these drifts.

The generation mechanisms of the long-term disturbance dynamo drifts is not clear. However, since there is strong evidence for appreciable changes in the composition of the low-latitude ionosphere about 1 day after large high-latitude current disturbances [e.g., *Fuller-Rowell et al.*, 1994, 1996], it is possible that these drifts result from the dynamo action of storm-driven composition/conductivity effects. These longer-term effects could also be partly due to electric fields resulting from the decay of the storm time ring current in the recovery phase of a magnetic storm (R. Wolf, private communication, 1997).

3.3. Ionospheric Disturbance Dynamo Model

In this section, we present our empirical model for the equatorial disturbance dynamo drifts developed using the methodology described in our companion paper. This model takes into account both short- and long-term disturbance dynamo effects with time delays of 1-12 and 22-28 hours, respectively. The short-term effects, however, are best represented using two parameters *AE* (1-6 hours) and (*AE* (7-12 hours) which take into account the average auroral current effects with time delays of 1-6 and 7-12 hours, respectively. The equatorial ionospheric vertical drifts, due to ionospheric disturbance dynamo electric fields, are then expressed as

$$V_d(t,AE) = \sum_{i=1}^{9} \{a_{i,3} AE_d(1-6 \text{ hours}) + a_{i,4}\, \alpha\, AE_d(7-12 \text{ hours}) + a_{i,5}\, \beta[AE_d(22-28 \text{ hours}) - 200 \text{ nT}]\} N_{i,4}(t) \quad (1)$$

where t is local time, $AE_d = AE - 130$ nT for $AE > 130$ nT and $AE_d = 0$ for $AE \le 130$ nT, α and β take into account the effects of shorter-term disturbance levels on the efficiencies of dynamo processes with time delays of 7-12 and 22-28 hours, respectively. These parameters, obtained by least square fits to the data, are given by

$$\alpha = \begin{cases} 0 & AE(1-6\text{hours}) < 200\text{nT} \\ \dfrac{AE(1-6\text{hours})}{100\text{nT}} - 2 & 200\text{nT} < AE(1-6\text{hours}) < 300\text{nT} \\ 1 & AE(1-6\text{hours}) > 300\text{nT} \end{cases} \quad (2)$$

and $\beta = \exp[-AE(1\text{-}12 \text{ hours})/90 \text{ nT}]$ for $AE(1\text{-}12 \text{ hours}) \ge 70$ nT, and $\beta = \exp[-70/90] = 0.46$ for $AE(1\text{-}12 \text{ hours}) < 70$ nT (see Figure 6). The last term on the right-hand side of (1) takes into account the linear increase of the long-term disturbance dynamo drifts for AE_d(22-28 hours) > 200 nT. This term is set

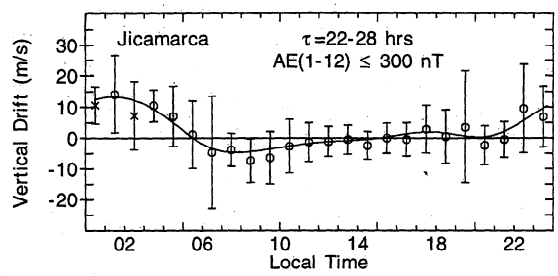

Figure 7. Local time variation of the long-term disturbance dynamo drifts for geomagnetically quiet short-term conditions. The crosses indicate averages from less than five data points.

Table 2. Disturbance Dynamo Model Coefficients (1-Hour Time Resolution)

B Spline	$a_{i,3}$	$a_{i,4}$	$a_{i,5}$, m/s nT
$N_{1,4}$	-0.0152	-0.0174	-0.0704
$N_{2,4}$	-0.0107	0.0152	-0.0674
$N_{3,4}$	-0.0132	0.0020	-0.0110
$N_{4,4}$	0.0095	0.0036	-0.0206
$N_{5,4}$	0.0085	-0.0140	0.0583
$N_{6,4}$	-0.0109	-0.0031	-0.0427
$N_{7,4}$	0.0086	0.0149	0.2637
$N_{8,4}$	0.0117	0.0099	0.3002
$N_{9,4}$	0.0338	0.0099	0.0746

to zero for AE_d(22-28 hours) ≤ 200 nT. The local time dependence of the vertical drifts is described by nine normalized cubic-B splines of order four, $N_{i,4}(t)$. Eight nodes were placed in equally separated local time intervals at 0,3,6,...,21 hours, and an additional node was placed at 4.5 LT to account for rapid changes near dawn. The coefficients of the model, given in Table 2, were obtained by a least squares fit to the entire database after removal of direct penetration effects using the model described in the companion paper by *Fejer and Scherliess* [this issue].

Figure 8 shows the model results for the three basic disturbance dynamo components considered in this study for AE_d = 400 nT over the three periods. The component with time delays of 7-12 hours is not shown separately since, as mentioned earlier, it is strongly affected by the shortest-term (1-6 hours) disturbance levels. For continuously disturbed conditions, the efficiency of the short-term effects increases up to time delays of about 12 hours between 2200 and 0800 LT, whereas in the late morning-early afternoon sector it maximizes after about 6 hours. The maximum upward drift perturbations associated with the short- and long-term disturbances occur at about 0400 and 0200 LT, respectively.

Figures 4 and 7 show comparisons of the model results with the binned data at different storm times. The corresponding average *AE* values are given in Table 1. It is important to note that these model results were obtained using as input parameters the hourly AE_d values of the binned data.

Several points should be kept in mind when comparing the model predictions with measured drifts. First of all, our model corresponds to the average disturbance conditions of our database (e.g., $AL/AU \approx 2$). As a result of the use of *AE* indices, we do not take into account effects associated with high-latitude energy deposition in different local time sectors. As pointed out by *Mazaudier and Venkateswaran* [1990], the assumption of longitude independent high-latitude heating can lead to large errors. In addition, our model does not consider a possible dependence of the disturbance dynamo drifts on season and solar cycle. If these effects are important, then our model should most closely represent moderate solar flux equinoctial disturbance drifts. We have also relied entirely on auroral indices from the northern hemisphere although the equatorial storm time ionospheric dynamo electric fields are driven by energy deposition in both the northern and southern hemispheres. As a result, we might underestimate these effects near December solstice and overestimate them near June solstice. The limitations resulting from the use of the *AE* index are discussed by *Fejer and Scherliess* [this issue]. Finally, there are probably additional effects not being taken into account in our model which could sometimes play important roles on the generation and time delays of low-latitude disturbance electric fields.

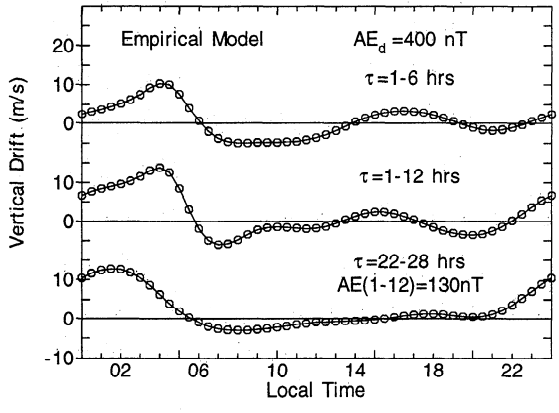

Figure 8. Plots of the basic disturbance dynamo drift components in our empirical model for values of the *AE* index of 400 nT above our quiet time level.

3.4. Case Studies

In this section, we present two examples of long-term disturbance dynamo effects. Additional examples which illustrate the occurrence of different disturbance drift processes and the limitations of our empirical models are presented in our companion paper.

Figure 9 shows again the auroral and equatorial measurements for the storm period of August 1972 but now together with the calculated disturbance dynamo and prompt penetration (the latter is discussed in our companion paper)

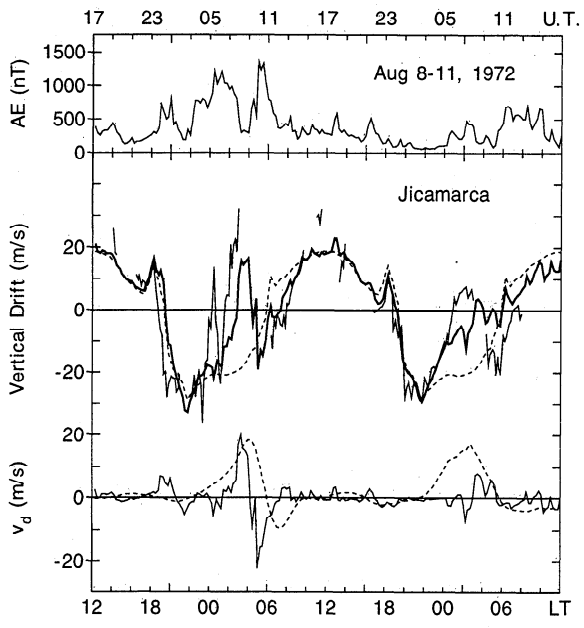

Figure 9. (top) Auroral electrojet indices; (middle) measured (thin solid line), quiet time (dashed line), and empirically modeled (thick solid line) vertical plasma drifts over Jicamarca; (bottom) and the prompt penetration (solid line) and the disturbance dynamo (dashed line) components of the vertical plasma drifts for August 8-10, 1972. The modeled vertical drifts shown in the middle were obtained by adding the average quiet time and the perturbation drifts.

drift components in the bottom panel, and the average quiet time and model predictions obtained by adding the perturbation and quiet time drifts in the center panel. The disturbance dynamo mechanism gives rise to perturbation drifts with time constants of a few hours following large enhancements in the high-latitude current system. For the period shown in Figure 9, our disturbance dynamo drift model can explain the large and long lasting nighttime perturbations on August 9-10, when the auroral indices indicated only very modest geomagnetic activity. This large departure from the quiet time pattern is due entirely to long-term disturbance dynamo drifts resulting from the large energy deposition into the high-latitude ionosphere about a day earlier. The large perturbation drifts between about 0100-0500 LT on August 9, when the *AE* indices showed large variations, were due to the combined effects of prompt penetration electric fields and short-term (1-6 hours) disturbance dynamo effects. Additional examples, and a more detailed discussion of the effects of prompt penetration electric fields, are given in our companion paper.

Figure 10 presents an additional example of equatorial plasma drifts during a period when very large auroral disturbances were immediately followed by very quiet geomagnetic conditions. In this case, largely depressed daytime drifts were observed during the morning of February 12. *Fejer et al.* [1983] attributed these anomalous electric field pattern to disturbance dynamo effects. Our model confirms this interpretation, although it underestimates the measured perturbations by a factor of about 2, which reflects the large variability of the efficiency of the long-term dynamo electric fields shown in Figure 6.

Finally, we should point out that, as expected, there are also a number of cases when our disturbance dynamo model is unable to explain the observations. One such case is that of January 12, 1988, when large high-latitude current disturbances were associated with the passage of a magnetic cloud. In this case, our model calculations predicted large nighttime equatorial upward velocity perturbations a day after the large auroral effects, but the Jicamarca observations did not show noticeable disturbances. We reiterate that our empirical model corresponds to the average conditions which characterize our database. The main limitations result from crude parameterization of the Joule heating at high-latitudes and from the day-to-day variability of the quiet time atmospheric dynamo electric fields. The detailed study of these and other important additional effects will require a larger database than is presently available.

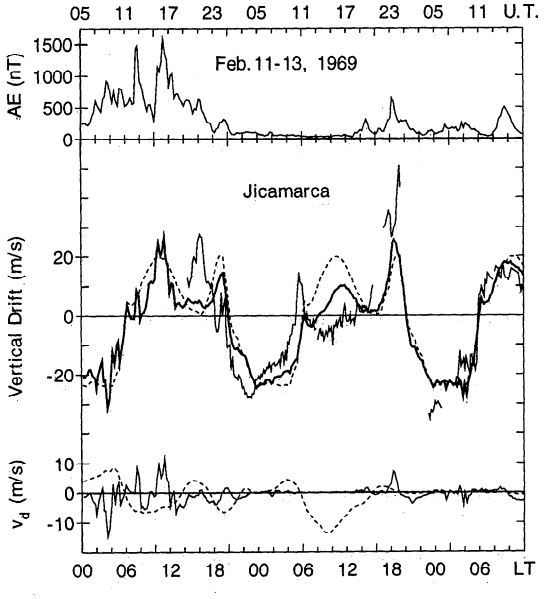

Figure 10. Same as Figure 9, but for the February 11-13, 1969 period. Notice that the negative daytime vertical drifts on February 12 occurred during a geomagnetically quiet period.

4. Conclusions

We have determined the average characteristics of the equatorial vertical plasma drifts driven by the ionospheric disturbance dynamo electric fields as a function of the time history of the auroral current activity determined from the *AE* index. These perturbation drifts, due to enhanced energy deposition into the high-latitude ionosphere, generally have short- and long-term components with time delays of 1-12 and 22-28 hours, respectively. The short-term disturbance dynamo generates upward vertical velocities at night and smaller downward velocities during the day which disappear about 6 hours after geomagnetic quieting. The long-term disturbance dynamo process generates upward velocities at night and downward drifts in the sunrise-noon period but only during magnetically quiet periods preceded by strongly active conditions. There is a complex interplay of disturbance dynamo electric fields with different timescales and large variability on the efficiencies of the different dynamo processes. This indicates the likely importance of other parameters such as the longitudinal distribution of the high-latitude energy deposition.

We have derived an empirical analytical model for the equatorial disturbance dynamo vertical drifts using a time series of the *AE* index as the input parameter. The short-term perturbation velocity pattern predicted by the model is in excellent agreement with that from the Blanc-Richmond disturbance dynamo model for a comparable energy input into the high-latitude ionosphere. Case studies often indicate good agreement between model predictions and observations but also confirm that additional effects such as the local time sectors of energy deposition in both high-latitude ionospheres, and the day-to-day variability also need to be taken into account for more accurate predictions.

Acknowledgments. We thank R. Wolf, R. Spiro, D. Hysell, E. Kudeki, A. Richmond, and M. Mendillo for useful discussions. This work was supported by the Aeronomy Program, Division of Atmospheric Sciences of the National Science Foundation through grant ATM- 9423479. The Jicamarca Radio Observatory is operated by the Instituto Geofisico del Peru, with support from the National Science Foundation.

The Editor thanks D. L. Hysell and G. W. Prölss for their assistance in evaluating this paper.

References

Ahn, B.-H., S.-I. Akasofu, and Y. Kamide, The Joule heating production rate and the particle energy injection rate as a function of the geomagnetic indices *AE* and *AL*, *J. Geophys. Res.*, *88*, 6275-6287, 1983.

Ahn, B.-H., Y. Kamide, H. W. Kroehl, and D. J. Gorney, Cross polar potential difference, auroral electrojet indices, and solar wind parameters, *J. Geophys. Res.*, *97*, 1345-1352, 1992.

Blanc, M., and A. D. Richmond, The ionospheric disturbance dynamo, *J. Geophys. Res.*, *85*, 1669-1688, 1980.

Denisenko, V. V., and S. S. Zamay, Electric field in the equatorial ionosphere, *Planet. Space Sci., 40*, 941-952, 1992.

Fejer, B. G., Equatorial ionospheric electric fields associated with magnetospheric disturbances, in *Solar Wind Magnetosphere Coupling*, edited by Y. Kamide and J. A. Slavin, pp. 519-545, Terra Sci., Tokyo, Japan, 1986.

Fejer, B. G., The electrodynamics of the low latitude ionosphere: Recent results and future challenges, *J. Atmos. Terr. Phys., 59*, 1456-1482, 1997.

Fejer, B. G., and L. Scherliess, Time dependent response of equatorial ionospheric electric fields to magnetospheric disturbances, *Geophys. Res. Lett., 22*, 851-854, 1995.

Fejer, B. G., and L. Scherliess, Empirical models of storm time equatorial zonal electric fields, *J. Geophys. Res.*, this issue.

Fejer, B. G., D. T. Farley, R. F. Woodman, and C. Calderon, Dependence of equatorial *F* region vertical drifts on season and solar cycle, *J. Geophys. Res., 84*, 5792-5796, 1979.

Fejer, B. G., M. F. Larsen, and D. T. Farley, Equatorial disturbance dynamo electric fields, *Geophys. Res. Lett., 10*, 537-540, 1983.

Fejer, B. G., R. W. Spiro, R. A. Wolf, and J. C. Foster, Latitudinal variation of perturbation electric fields during magnetically disturbed periods: 1986 SUNDIAL observations and model results, *Ann. Geophys., 8*, 441-454, 1990.

Freund, J. E., and R. E. Walpole, in *Mathematical Statistics*, pp. 473-480, Prentice-Hall, Englewood Cliffs, N. J., 1987.

Fuller-Rowell, T. J., M. V. Codrescu, R. J. Moffet, and S. Quegan, Response of the thermosphere and ionosphere to geomagnetic storms, *J. Geophys. Res., 99*, 3893-3914, 1994.

Fuller-Rowell, T. J., M. V. Codrescu, H. Rishbeth, R. J. Moffet, and S. Quegan, On the seasonal response of the thermosphere and ionosphere to geomagnetic storms, *J. Geophys. Res., 101*, 2343-2353, 1996.

Mazaudier, C. A., and S. V. Venkateswaran, Delayed ionospheric effects of the geomagnetic storms of March 22, 1979 studied by the sixth coordinated data analysis workshop (CDAW-6), *Ann. Geophys., 8*, 511-518, 1990.

Mazaudier, C. A., A. D. Richmond, and D. Brinkman, On thermospheric winds produced by auroral heating during magnetic storms and associated dynamo electric fields, *Ann. Geophys., 5*, 443-448, 1987.

Prölss, G. W., Ionospheric *F*-region storms, in *Handbook of Atmospheric Electrodynamics*, vol. 2, edited by H. Volland, pp. 195-248, CRC Press, Boca Raton, Fla., 1995.

Reiff, P. H., The use and misuse of statistics in space physics, *J. Geomagn. Geoelectr., 42*, 1145-1174, 1990.

Senior, C., and M. Blanc, On the control of magnetospheric convection by the spatial distribution of ionospheric conductivities, *J. Geophys. Res., 89*, 261-284, 1984.

Spiro, R. W., R. A. Wolf, and B. G. Fejer, Penetration of high-latitude electric field effects to low latitudes during SUNDIAL 1984, *Ann. Geophys., 6*, 39-50, 1988.

Woodman, R. F., Vertical drift velocities and east-west electric fields at the magnetic equator, *J. Geophys. Res., 75*, 6249-6259, 1970.

B. G. Fejer and L. Scherliess, Center for Atmospheric and Space Sciences, Utah State University, Logan, UT 84322-4405. (e-mail: bfejer@cc.usu.edu)

(Received May 30, 1997; revised July 22, 1997;
accepted July 24, 1997.)